GusT

Randy Chang
Luis Garcia
Robin Liu
Matt Notary
Bob Perez
Harris Yong

GUST

MAE 321: Engineering Design

-Team A-
Randy Chang
Luis Garcia
Robin Liu
Matt Notary
Bob Perez
Harris Yong

12 Jan 1999

TABLE OF CONTENTS

GusT

MAE 321: Engineering Design

-Team A-

Randy Chang

Luis Garcia

Robin Liu

Matt Notary

Bob Perez

Harris Yong

12 Jan 1999

EXECUTIVE SUMMARY

GusT is a compact, high power leaf blower prototype designed to operate with a much lower noise level than those currently in production. The prototype model yielded a 31 m/s (68 mph) discharge velocity and a 0.09 m^3/s (196 ft^3/min) flow volume. This was achieved while still maintaining a compact shape(see Table 1)weighing under 3.6 kg (8 pounds). Most importantly, GusT produced a peak operational noise of no higher than 90dBA when measured at a distance of one meter while in operation. This change represents a 8dBA reduction compared to current leaf blowers with similar specifications. Simply stated, peak noise has been reduced by nearly a factor of 6. Gust is designed mainly for the homeowner, but key design elements used in noise reduction can easily be incorporated in an industrial-grade unit suitable for the professional gardener. While its compact, lightweight design makes the unit easily portable and the high power output is more than enough to move wet leaves and other common lawn debris, it is the reduced noise that is most critical.

Several communities have recently placed bans on the use of leaf blowers because they are excessively noisy. Cities such as Los Angeles have passed ordinances prohibiting the use of certain types of leaf blowers because they are "…loud…obnoxious…[and]…ruin all or part of every fall weekend" (Queenan 70). Other areas do not allow the use of leaf blowers above a certain noise level or restrict the times during which leaf blowers can be operated. Therefore, the main design philosophy in developing GusT was to make it quiet.

The design concept used in GusT focuses on reducing fan and motor noise by lowering the shaft's rotational speed. Current designs have motors that spin at approximately 15,000 rpm. In order to achieve the velocity and flow rates of the target specifications at a reduced motor rpm, GusT is built in a two-stage, serial axial fan design. By placing the two fans serially, similar performance necessary to achieve the target specifications for velocity and volume flow can be met the 7000 rpm operational speed. In a further effort to lessen the noise, sound-absorbing material is also used to house the fan and motor.

-Team A-
Randy Chang
Luis Garcia
Robin Liu
Matt Notary
Bob Perez
Harris Yong

INTRODUCTION

Objectives, Specifications & Constraints

Discharge velocity	31	m/s	68	mph
Volume flow rate	0.09	m^3/s	196	ft^3/min
Operating speed	7350	rpm	7350	rpm
Length	1	m	40	in
Diameter	0.2	m	8	in
Weight	~3.6	kg	~8	lb

Table 1: Key performance specifications

The objective of the Quiet Leaf Blower project is to design and manufacture a small, quiet, yet powerful leaf blower that can be competitively marketed internationally. GusT is primarily targeted at homeowners, with the possibility of a second, more powerful gardening variation in the future. Since the unit is intended for personal yard maintenance, it must be both portable and ergonomic. This means volume, weight, portability, durability, simplicity, and appearance must all be factored into the final design.

GusT performance and price should be similar to that of a Toro Electric Super Blower Vac, Model 51587, with a noise output that is 20dBA less than the Toro's. The final requirement is that initial prototyping costs be limited to $300.

Research Findings

- ### Common Fan Designs and Tradeoffs

A generic survey of current products finds that almost all available leaf blowers are based on a radial pump design. This may be due to the fact that a properly designed radial pump can produce a large pressure gradient fairly compactly. In terms of fan noise, a backward swept radial fan is among the quietest pumps available.

Whereas the applications of both radial and axial designs do overlap, axial flow pumps are generally better suited for applications requiring high volumetric flow rates, whereas radial designs tend to produce more head.

Partly because axial flow designs do not necessitate a volute to redirect the flow, axial pumps have higher efficiencies. However, these higher efficiencies are often difficult to realize because swirl is a significant problem with axial fans. In an ideal axial flow situation, fluid leaving the fan blade is normal to the exit plane. In reality, the blades exert a torque on the flow, creating a velocity component that is not along the axis of the duct. Since not all the flow is directed out of the nozzle, useful kinetic energy is lost in this swirling motion. Common methods for recovering this lost energy include vanes, stators and counter-rotating fans, where the latter method has 2 fans rotating in opposite directions. The second fan then effectively cancels the swirl generated by the upstream fan. It is possible to achieve a 10% efficiency increase with this type of design.

Stators and vanes are essentially fixed fans that redirect airflow. When properly shaped, stators redirect the swirled air until it is parallel to the duct axis. Unfortunately, calculating the correct stator angles is quite difficult. Industry typically uses tufts and models as opposed to purely analytical methods to determine these angles.

Although fan output is a strong function of its rotation rate, fans can be serially staged or placed in parallel to increase performance. Serial designs increase head significantly while parallel designs offer high flow rates.

- ### Duct & Housing Considerations

Although a contracting duct is necessary to increase the exit velocity, the cross sectional area cannot decrease too quickly or the flow will separate, leading to significant losses.

Similarly, there should be minimal bends and sharp curves. If these curves are necessary, there should be a significant passage of purely straight flow before reaching the fans. The intake should be as unobstructed as possible to minimize throttling effects and pressure changes prior to the fan.

- ***Noise***

GusT's noise level will be measured using an A-weighted sound spectrum. Modern machinery generates sound waves over a spectrum of frequencies. Fortunately, the human ear only amplifies signals between several hundred HZ to several Hz. Any waves beyond these frequencies are less audible. The A-weighted scale is effectively a transfer function (Equation 1a) and reflects the gain perceived by the human ear. Unfortunately, this does not mean humans are immune to signals whose fundamental frequency is beyond human hearing. Noise from most types of common machinery contains harmonics and subharmonic audible signals.

Equation 1a. dBA scale transfer function.

$$A(f) = \frac{12200^2 * f^4}{(f^2 + 20.6^2)*(f^2 + 12200^2)*\sqrt{f^2 + 107.7^2 * \sqrt{f^2 + 737.9^2}}}$$

$$dBA(f) = 20 * \log\left(\frac{A(f)}{A(1000)}\right)$$

Equation 1b. dBA scale normalization.

The source of noise in any leaf blower is the motor. Reducing revolution speed or decreasing the fan radius can reduce motor noise. Unfortunately, both of these methods reduce the pump's volumetric flow rate. Blade size can be increased to counteract this effect, but portability restricts the maximum blade size. In order to decrease the noise, then, the motor revolution speed must be decreased. A slower fan rotation, though, will also limit the flow velocity.

Other sources of noise are the fan tips, inlet, and exit. Designing a housing with a larger tip clearance can decrease fan tip noise. The larger area prevents turbulent air from becoming trapped between the blade tips and housing. Unfortunately, increasing tip clearance has the negative effect of decreasing efficiency. Inlet and exit noise can be reduced by wrapping soundproofing material around the duct.

-Team A-
Randy Chang
Luis Garcia
Robin Liu
Matt Notary
Bob Perez
Harris Yong

DESIGN CONCEPTS AND FEATURES

Basic Design

After considering the strengths and weaknesses of several designs, an axial flow design was chosen as the most suitable. GusT uses a dual-stage, axial flow pump to displace a proven 0.09 m^3/s at an exit velocity of 31 m/s. The original design called for 2 stators to be placed before the first and second stage. However, preliminary testing showed the net effect of these stators was to obstruct the flow. It was more efficient to redesign the second fan to account for a flow angle out of the second stage rather than implementing a suitable stator due to a highly radial component of flow exiting the first rotor. The two co-axially mounted fans are approximately 20 cm in diameter and are designed for optimal performance around 7,000 rpm.

The duct of GusT begins with a circular cross section to house the fans and then tapers to an ellipse. This design was chosen over a regular contraction because the change to the small elliptical outlet decreases the effect of swirl. When a swirling flow leaves the fan blade, it continues to rotate through the cylindrical passage. Flattening the nozzle's cross section into an ellipse breaks up this swirling pattern. Furthermore, the flattened shape is more efficient since more flow is directed along the ground's contours rather than above it.

GusT prototypes were built with inexpensive, workable PVC plastic and Styrofoam. The axial fans and duct supports were fabricated from the plastic and the duct was produced out of Sytrofoam. Both materials were machined using a 3-axis CNC mill. Purchase requirements included the motor, bearings, keyed shaft, and coupling.

An electric motor was chosen for its advantage over an internal combustion engine in simplicity, noise, pollution, and weight.

Production Model Design Concept

As seen in figure 1-4, GusT features a futuristic design that will attract the buyer's attention right off the shelf. The fans and motors are enclosed in a streamlined casing which is circular in cross section. After the fans, the duct contracts and the cross section changes to an ellipse at the exit of the blower. The main handle comes out from casing at the top of the inlet. The second handle stems from midway down the duct and features an interlocking design which allows this handle to be rotated around the circumference of the casing. This unique feature makes GusT user friendly to both right and left handed people, and was one of the driving factors behind this design. The streamlined shape of GusT was dictated by the desire for an aerodynamic, sleek design that is an extension of the body, not a blunt, cumbersome garden tool. Furthermore, the design meets the consumers' demands of a light-weight, easily stored and portable leaf blower. Notably, the T-shaped handle on top of the main handle allows GusT to be easily carried. A supplementary shoulder strap will also be included to facilitate

Figure 1. Isometric View

-Team A-
Randy Chang
Luis Garcia
Robin Liu
Matt Notary
Bob Perez
Harris Yong

12 Jan 1999

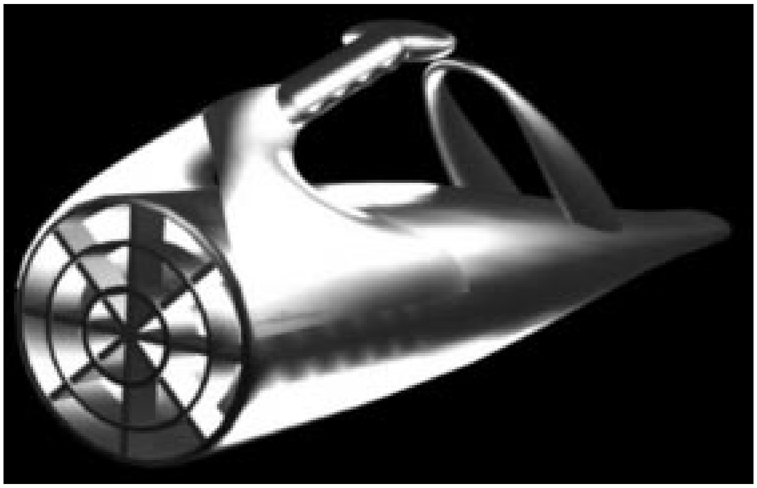

Figure 2. Back view

usage. These features are bound to revolutionize garden tool aesthetics.

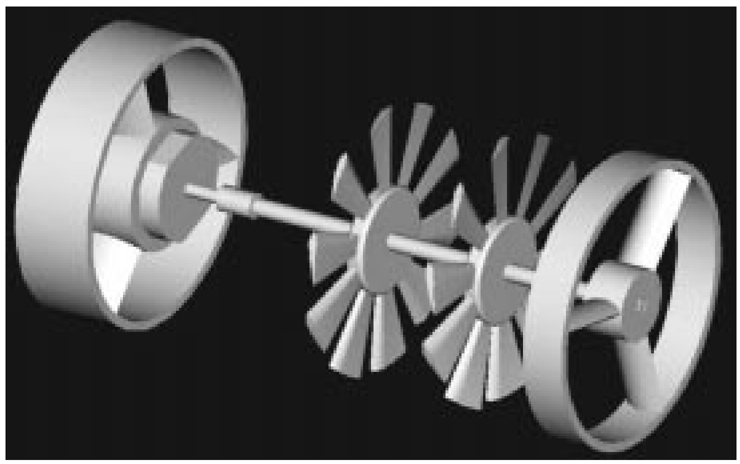

Figure 3: GusT internal schematic. Note that the finned hubs at each end of the shaft are actually duct supports. Themotor is encased in the rear support.

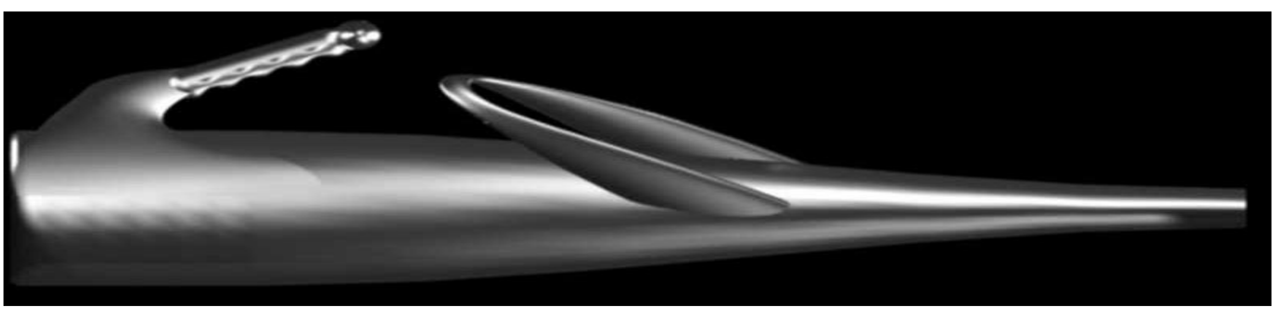

Figure 4. Side view.

-Team A-
Randy Chang
Luis Garcia
Robin Liu
Matt Notary
Bob Perez
Harris Yong

12 Jan 1999

Design Decision Rationale

The driving force behind most design decisions was noise reduction; GusT utilizes many means of achieving low noise. Reducing shaft speed is the most important because the fan and motor are the main source of noise. The prototype GusT is designed to yield optimal performance at 7,000 rpm, less than half the industry norm of 15,000 rpm. Slightly larger fan blades are used to compensate for the slower shaft speed, but this feature alone is insufficient. Therefore, GusT boasts the benefit of serial staging. By having two coaxially mounted fans, head and flow rate, can be increased without the need to resort to higher rotational rates or fan dimensions. This allows GusT to benefit from reduced high pitch motor and fan noise while still maintaining a high enough fan rotation rate for sufficient head and flow.

Whereas parallel staging can also increase performance, the high exit velocities required by a leaf blower result in a steeply rising system head curve. As a result, a pressure additive serial system is more effective than a flow additive parallel system. Although axial fans tend to produce less pressure rise, they can be easily staged to create larger pressure gradients, especially since the long duct easily accommodates multiple rotors. Thus It is clear that the inherent disadvantages of an axial design disappear when multi-stage designs are considered.

Mechanical complexity has also been considered in the design process. While axial fans can be serially staged simply by mounting fans coaxially on a shaft, radial fans cannot be designed in series without incurring complex geometries to redirect the flow between stages. Furthermore, a complex shaft design that increases weight and complexity is necessary to drive two serial radial pumps since the pumps rotate in orthogonal planes. Even with single stage designs, a radial pump is rather complex. In particular, the shape of the volute is critical in determining pump performance. Since the fluid undergoes right angle turns, flow direction is very complex, resulting in generally lower efficiencies than well-designed axial configuration.

Nevertheless, an argument can still be made for radial designs. However, in order to achieve the necessary pressure increase to sustain the specified discharge velocity and flow volume at low rotational speeds, a staged design is necessary. Initially, a double-sided radial fan drawing air from both sides was considered. But since as the system curve for a high discharge velocity leaf blower is steep, serial staging is preferred. However this is too mechanically complex if radial pumps are specified. Also, because serially staged radial pumps require two air intakes in two orthogonal planes, the use of space is inefficient and throttling losses can occur with poorly designed inlets. The axial system is basically a straight-through design, where the intake, the fans, and the exit are coaxial. Another possible design is a pair of counter-rotating fans. This design has advantages in efficiency and some noise cancellation effects. Counter-rotating shafts, planetary gearsets or bevel gears can be used to produce rotations in opposite directions. However, these designs were deemed too mechanically complex for a leaf blower. It would be too delicate to endure the impacts and weathering endured by most gardening equipmen. Therefore, the current design rotates 2 axial fans in the same direction.

Manufacturing & Cost Analysis

Cost and ease of assembly is another area in which GusT is holds an advantage over the competition. Since all major components are coaxially mounted to the main shaft, GusT can be assembled much faster than competing designs. This attribute roved advantageous during prototype development when GusT was the first designs to be fully assembled and ready for initial testing. In addition, the advantage of a simple design will be most useful during full scale manufacturing where fewer assembly hours will be required on the assembly

-Team A-
Randy Chang
Luis Garcia
Robin Liu
Matt Notary
Bob Perez
Harris Yong

12 Jan 1999

line. In addition, the coaxial design gives GusT an advantage on the manufacturing floor since assembly machines will not have to be arranged for multi-axis assembly. Higher production efficiencies will maximize per unit profit margins as well as undercut the competition.

GusT also benefits from a simple, elegant layout requiring a minimum number of parts. No additional gears, belts, or other cluttering assemblies are used in achieving its performance. This simple, yet rugged design will also allow GusT to survive expected abuse during its operational life span. The effect of weather, impact, and extreme temperature differences will have a minimal effect on GusT.

Production models will use roughly equal quantities of plastic as leaf blowers already on the market. The most expensive piece of equipment will be the motor. Other costs will include plastic for the blades and housing. A nominal price will also be paid for the keyed shaft, coupling, and self-aligning bearings. The area where GusT will post a cost advantage is in assembly costs. The axial layout is much simpler to assemble than competing Quiet Leaf Blower prototypes. Using mass production prices, the total production cost should not exceed $30.

DETAILED DESIGN AND ANALYSIS

The analysis and design procedure for axial fan blades is addressed here. It is recognized that a dual stage serial axial design will yield a more substantive press ure rise, but a rigorous treatment of such a configuration is omitted from this analysis. The present analysis reflects a robust model for a single stage rotor. Approximations regarding incoming and exiting flow angles and velocities at the blade tips are prominent throughout the analysis to reduce iterative processes between dependent parameters.

Operating Speed	ω	7000	rpm
Fan (general)			
Hub radius	rin	0.038	m
Tip radius	rout	0.095	m
Blades			
NACA 0015 (reinforced at hub)			
Duct			
Largest duct area	A1	0.032	m^2
Smallest duct area	A2	0.003	m^2
Upstream Fan			
Static angle of attack at hub	αin1	16	°
Static angle of attack at tip	αout1	14	°
Nominal true angle of attack	ϕ1	13	°
Downstream Fan			
Static angle of attack at hub	αin1	11	°
Static angle of attack at tip	αout2	9	°

Table 2: Actual performance specifications

Noise output of a leaf blower is most strongly dependent on the rotational speeds of the motor and fan, but GusT succeeds in reducing the required speed of rotation with little compromise of head and flow. Pressure increase across the rotors is achieved through dual staging (with two coaxial rotors) as well as the use of larger fan radii.

GusT design is powered by a motor capable of 7000 rpm operation. Lower rotational speed and torque requirements should allow for a smaller, more streamlined motor than those currently in production.

GusT design was parameterized to allow for the shifting of parameters governing the flow behavior (angles, velocities, losses, etc.) in order to reach an optimal operating point. Refer to the chosen design parameters in Table 2 for current values. The duct contraction area ratio is chosen to allow for nearly a ten-fol increase in flow velocity through the reduction of duct area, while avoiding flow separation through a smooth contraction governed by a shallow 18° convergence.

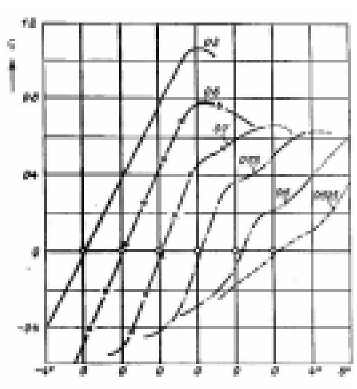

Figure 5. Lift curves as a function of angle of attack and Mach number (Riegels).

Refer to Table 2 for the design specifications of the fan blades. The chosen blade is the NACA 0015 model, with a slight modification at the hub for structural integrity. A Mach Number of 0.3 was determined for flow through the fan, and the corresponding lift curve was chosen appropriately (Figure 5). Additionally, there is a 1.6 cm total clearance for the fan tips.

The analysis assumes a fan rotational speed of 7,000 rpm or about 733 rad/s, a significant reduction from the 15000 rpm drive used by the competition. Although increasing the number of blades increases the pressure gain of the fan, the increase is not without cost because cascading interference effects come into play significantly as the stagger angle (the angle between the blades) reduces to below 50° (Hay). GusT has 10 blades per rotor, or 40° of stagger angle. With these values, the solidarity of the fan (blade pitch to chord length ratio) is about 1.4.

-Team A-
Randy Chang
Luis Garcia
Robin Liu
Matt Notary
Bob Perez
Harris Yong

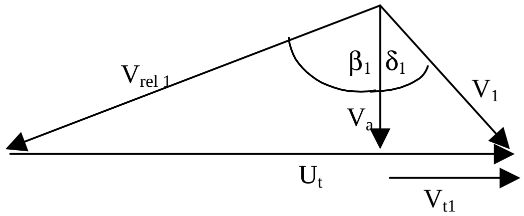

Figure 6a. Incoming flow velocity triangle.

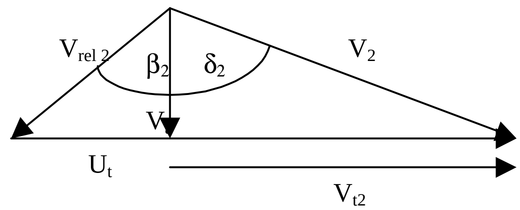

Figure 6b. Outgoing flow velocity triangle.

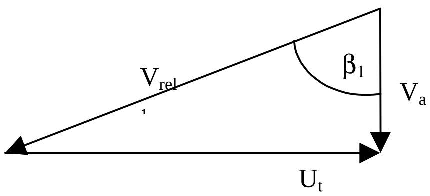

Figure 6c. Incoming flow velocity triangle assuming purely axial incoming flow.

$$P_{blade} = \frac{\int_{r_{in}}^{r_{out}} dFa}{\pi(r_{out}^2 - r_{in}^2)}$$

Equation 2. Pressure rise per blade.

$$dFa(r) = C_L \sin\phi - C_D \cos\phi q(r)c(r)dr$$
$$dFt(r) = C_L \cos\phi - C_D \sin\phi q(r)c(r)dr$$

Equation 3 a, b. Differential blade forces in the axial and tangential directions.

$$c(r) = chord_{out} \cdot \left(1 - (1-\lambda) \cdot \frac{(r_{out} - R)}{r_{out}}\right)$$

Equation 3c. Chord as a function of radius.

$$q(r) = \frac{1}{2}\rho V_{rel}^2 \approx \frac{1}{2}\rho V_{rel1}^2$$

Equation 3d. Dynamic pressure on blade.

$$\lambda = \frac{chord_{in}}{chord_{out}}$$

Equation 3e. Ratio of chords.

$$\beta = a\tan\left[\frac{U_t}{V_{a)}}\right] = a\tan\left[\frac{\varpi R}{V_a}\right] = a\tan\left[\frac{\varpi R}{Q/A_1}\right]$$

Equation 4. Relative velocity angle,.

At this point, a review of the velocity triangle concept is helpful. Figure 6 shows the typical velocity triangle shapes, where subscript 1 refers to velocities at the leading edge of a blade, and subscript 2, the trailing edge. Figure 6c shows a simplified velocity triangle for the leading edge when the incoming flow is assumed to be completely in the axial direction (V_{t1} is zero). U is the tangential velocity caused by the rotating rotor, V refers to the absolute velocity of the flow, while V_{rel} is the velocity relative to the blade on the rotor. V_a is the axial component of the velocity and is assumed to be constant as a result of the physical requirement for continuity.

The pump head, which ultimately defines the velocity and flow of GusT, is the change in static pressure that is produced by the rotors (P_{blade}, Equation 2), normalized by ρ and g to get an effective head with a length dimension. The blade element and free vortex theories are used to determine this P_{blade}. From geometry, it can be seen that the differential force per blade (in both the axial and tangential directions) is as shown in Equation 3a and 3b, where c(r) is the chord (Equation 3c), and q(r) is the average dynamic pressure (Equation 3d). In reality, q(r) is somewhat higher because the dynamic pressure leaving the trailing edge is higher due to the tangential velocity V_t that the rotating fan imparts. Figure 5 shows the important velocity components and angles. Equations also shows the lift and drag force on each blade.

For all occurrences of β, β is taken to be β_1, which is defined by Equation 4 and shown in Figure 6c. Ideally, a β_{mean} should be used, but this requires the value of V_{t2}, which needs to be iterated. Since the value of β_1 is the maximum possible β (a result of no tangential velocity), the true β_{mean} would be lower than the β_1. Therefore, the inaccurate β_1 affects many of the calculated values.

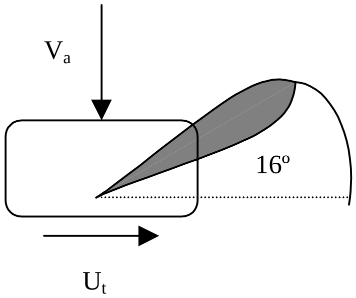

Figure 7a. Blade orientation of first fan at hub. Second fan has 5° less angle.

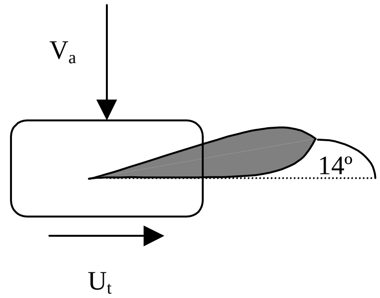

Figure 7b. Blade orientation at tip. Second fan has 5°less angle.

$$\alpha = \alpha_i + \left(\frac{Twist * R}{3R_{out}} * \frac{1+2\lambda}{1+\lambda}\right)$$

Equation 5. Static angle of attack, accommodating for twist.

$$\phi = \alpha - \left(\frac{\pi}{2} - \beta\right)$$

$$\phi = \alpha + \beta - \frac{\pi}{2}$$

Equation 6. True angle of attack.

Another important angle is ϕ, the actual angle of attack due to the rotation of the rotor as well as the incoming axial flow. ϕ is defined in Equation 6 and is dependent on the radius, among other parameters. GusT is designed with twist to accommodate the change in ϕ that would otherwise occur as a function of radius; without blade twist, ϕ would decrease with increasing radius, reducing lift at the tips while stalling the section closer to the hub. Care has been taken to determine a twist and an initial attack angle α_i, for operation at 7,000 rpm. The expression for twist is depicted as Equation 5. α_i was initially 11° at the hub to maintain a conservative true angle of attack of about 8° throughout the radius (Figure 7). However, it was found that the inaccuracies in our assumptions meant that these angles were overly conservative; α_i was thus increased to 16° for the first fan, while the 2nd stage remained at 11°. With the given values of α_i and twist, the blades on the first fan is mounted on the hub at an angle of 16° to the cross-section of the duct, reducing to 14° at the tips (Figure 7). The second stage has a corresponding design, with 5° less angle.

The blade force differential (Equation 3a) is integrated over the radius, and when normalized by the annular area swept by the fan yields the pressure rise (Equation 7). This pressure rise is multiplied by 10 to obtain the change in pressure given by the 10 blades. As mentioned earlier, these cascaded blades may result in a loss of efficiency per blade due to interference. However, from Hay, this loss is minimal for our solidarity and stagger angle. This head curve for one rotor as well as that for the dual stage system is plotted in Figure 8. With the above assumptions, an equation for the pump head curve can be explicitly written as shown by Equation 7.

$$\mathrm{Pump\_2\_stage}(Q) := \int_{Rin}^{Rout} \left[-Cd \cdot \frac{\frac{Q}{A1}}{\left[(\omega \cdot r)^2 + \left(\frac{Q}{A1}\right)^2\right]^{\frac{1}{2}}} - -2 \cdot \pi \cdot \left[Tw \cdot r \cdot \frac{1 + 2\cdot\lambda}{3 \cdot Rout \cdot (1+\lambda)} + \alpha i + \beta coeff \cdot \mathrm{atan}\left[\omega \cdot \frac{r}{\left(\frac{Q}{A1}\right)}\right] - \frac{\pi}{2} \right] \cdot \frac{\omega \cdot r}{\left[(\omega \cdot r)^2 + \left(\frac{Q}{A1}\right)^2\right]^{\frac{1}{2}}} \right] \cdot \frac{1}{2} \cdot \rho \cdot \left[\left(\frac{Q}{A1}\right)^2 + (\omega \cdot r)^2\right] \cdot Chordout \cdot \left[1 - (1-\lambda) \cdot \frac{Rout - r}{Rout}\right] dr \cdot 2 \cdot \frac{N \cdot Stages}{\pi \cdot \left(Rout^2 - Rin^2\right) \cdot \rho \cdot 9.8}$$

Equation 7. Head produced by two axial fan rotors.

A plot of the system curve is also necessary in determining the actual operating point of GusT. The system curve is derived directly from the continuity equation (Equation 8a) and two Bernoulli equations, upstream and downstream (Equation 8b); in addition, the frictional losses due to the interaction with the duct wall, and the losses that result from the duct contraction were accounted for. Further discussion on losses appears later. The full system curve is shown as the parabolic line in Figure 8, with its functional form appearing as Equation 9. This curve's dependence on V_2 is also apparent, which necessitates the calculation of the tangential and axial components of V_2. The axial component can be approximated as V_1 from continuity. V_{t2} can be determined by angular momentum conservation, shown in Equation 8c. However, this requires T, the torque generated by the blades, which is in itself dependent on V_{t2}. The integral in Equation 10 shows the determination of V_{t2}. The system curve plotted is defined by Equation 9 when the necessary substitutions are made.

-Team A-
Randy Chang
Luis Garcia
Robin Liu
Matt Notary
Bob Perez
Harris Yong

GUST

MAE 321: Engineering Design

-Team A-

Randy Chang

Luis Garcia

Robin Liu

Matt Notary

Bob Perez

Harris Yong

12 Jan 1999

$$\mathrm{Hsystotal}(Q) := \frac{1}{9.8\cdot 2}\cdot\left[\left(\left(\frac{Q}{A2}\right)\right)^2 - (V2(Q))^2 + \left(\frac{Q}{A1}\right)^2\right] + \left[\left[0.025\cdot\frac{0.7}{(2\cdot r2)} + 0.02\right]\cdot\frac{Q^2}{2\cdot 9.8\cdot A2^2}\right]$$

Equation 9. Total system curve equation.

$$\mathrm{Vt2}(Q) := \int_{\mathrm{Rin}}^{\mathrm{Rout}} \left[2\cdot\pi\cdot\left[\mathrm{Tw}\cdot r\cdot\frac{1+2\cdot\lambda}{3\cdot\mathrm{Rout}\cdot(1+\lambda)} + \alpha i + \beta\mathrm{coeff}\cdot\mathrm{atan}\left[\omega\cdot\frac{r}{\left(\frac{Q}{A1}\right)}\right] - \frac{\pi}{2}\right]\cdot\frac{\frac{Q}{A1}}{\left[(\omega\cdot r)^2 + \left(\frac{Q}{A1}\right)^2\right]^{\frac{1}{2}}} - \mathrm{Cd}\cdot\frac{\omega\cdot r}{\left[(\omega\cdot r)^2 + \left(\frac{Q}{A1}\right)^2\right]^{\frac{1}{2}}}\right]\cdot\frac{1}{2}\cdot\rho\cdot\left[\left(\frac{Q}{A1}\right)^2 + (\omega\cdot r)^2\right]\cdot\mathrm{Chordout}\cdot\left[1-(1-\lambda)\cdot\frac{\mathrm{Rout}-r}{\mathrm{Rout}}\right]\,dr\cdot\left(\frac{\mathrm{N}\cdot\mathrm{Stages}}{\rho\cdot Q}\right)$$

Equation 10. Determination of V_{t2}.

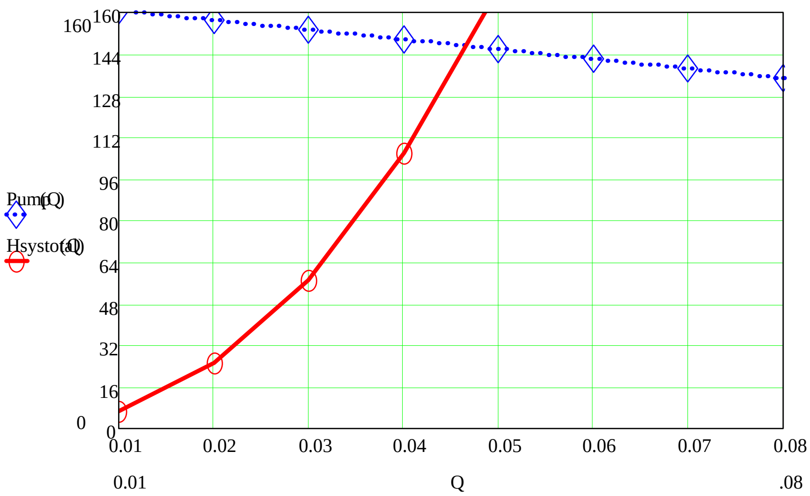

Figure 8: System Curve

$$\dot{m} = Q = A_1V_1 = A_2V_2$$

$$V_a = V_1 = \frac{Q}{A_1}$$

Equation 8a. Continuity equation.

$$p_{atm} = p_1 + \frac{1}{2}\rho V_1^2$$

$$p_2 + \frac{1}{2}\rho V_2^2 = p_{atm} + \frac{1}{2}\rho V_{ex}^2$$

Equation 8b. Bernoulli's equations upstream and downstream of fans.

$$T = \rho Q(R_2V_{t2} - R_1V_{t1})$$

$$V_{t1} = 0$$

$$V_{t2} = \frac{T\rho Q}{R}$$

$$T_{blade} = \int_{r_{in}}^{r_{out}} r\cdot dF_a$$

Equation 8c. Derivation of V_{t2}.

Frictional losses were calculated by this following procedure: From the flow characteristics, the Reynolds number was obtained, and the friction factor was determined. using an empirical relation, Equation 11. This equation approximates the transition and turbulent regions of the Moody diagram, which relates the friction factor to the Reynolds number and material roughness. The roughness of the plastic duct is assumed to be 0.1 mm; the characteristic length used is the smallest diameter of the duct. In addition, the total loss coefficient for the area contraction along the duct is found to be 0.02. The angle of the contraction is about 18°, and this 0.02 value is for a 30° contraction, so the actual losses should be less than that indicated. The friction factor and the loss coefficient were included in the system demand equation in order to properly account for the losses inherent in the design. The losses in the duct add the term shown in Equation 12 to the system curve.

$$H_{loss} = \left(f\frac{L}{D} + \sum K\right)\frac{Q^2}{2gA_2^{\,2}}$$

Equation 11. System head losses.

$$f = \frac{1.325}{\ln\left(\frac{\varepsilon}{3.7D} + \frac{5.74}{\mathrm{Re}^{0.9}}\right)^2}$$

Equation 12. Duct friction factor.

PROTOTYPE TESTING

FIRST ITERATION

The first GusT iteration was tested on December 11, 1998 using 2 identical axial fans and 2 stators. Two flexible sheets of polyurethane were rolled into a cylinder and a tapered cone to create the main housing and nozzle. Due to time limitations, flow angle exiting the first stage could not be measured sufficiently in advance to create a unique second fan. It was assumed the flow would enter the second stage parallel to the main axis after being straightened by the stator. Unfortunately, this was not the case. Incoming second stage flow still possessed enough swirl to exert a significant force on the fan blades. This design flaw was revealed when 3 fan blades broke off of the second stage hub at 3000 RPM. At this point, the decision was made to continue testing with the damaged second fan. The remaining blades in the second stage broke off at 6000 RPM, leaving a bare hub in the second stage. At this point single stage performance was evaluated using the remaining first stage. The first round of tests ended when the shaft de-coupled at 6600 RPM.

Plotting dynamic pressure vs. RPM showed that single stage operation yielded larger pressures than dual stage operation. This suggested that the second stage, which was poorly designed, obstructed flow rather than increasing it. Subsequent iterations took incoming flow angle into account for designing the second fan.

First iteration testing revealed GusT's main weakness: noise. The plot of Noise vs. RPM shows that a considerable amount of noise was being generated. A large portion of this noise was due to mechanical vibration and resonance; therefore, tighter manufacturing tolerances can produce some noise reduction. Also, a notable amount of noise was produced by extra material rattling on the table. During actual testing the table will be cleared of all non-essential equipment to eliminate this noise source.

A comparison of theoretical and experimental single stage performance shows mixed results. Actual volumetric flow was close to theoretical estimates. However, head was much lower than expected, indicating the net effect of the fan blades was to produce negative lift. Optimizing the second stage and revising duct design should alleviate this problem.

SECOND ITERATION

After first iteration testing, two factors that limited GusT's performance became apparent. First, poor balancing of the motor and fans led to severe vibration that made GusT unsafe at high speeds. It was obvious that the silicone supporting the motor, although damping some vibration, was not effective enough. Abrasion marks on the self-aligning bronze bearings were caused by significant shaft wobble. For the second iteration, meticulous effort was paid to balancing all rotating machinery. A keyed, stainless steel shaft was purchased; in addition, new heavy-duty shaft and motor mounts were manufactured in order to cut down on motor vibration. The second iteration also includes a styrofoam duct for better sound absorption.

The second obvious problem was that the second stage constricted flow. This problem occurred because the second stage was essentially a repeat of the first stage. Once an operational first stage became available, flow angles were calculated for a new second stage. It should also be noted that the first stage did not meet the flow conditions exactly; the blades of the first stage were designed to see flow at 10000 rpm and 0.1m^3/s, well above that tested due to vibrational limitations. As a result of these limitations, operational speed has been reduced to 7,000 rpm in the second iteration; both fans have been redesigned to yield maximum head and flow at the slower speed. In addition, the blade cross-sectional area has been increased in order to provide sufficient structural integrity for high speed operation.

-Team A-
Randy Chang
Luis Garcia
Robin Liu
Matt Notary
Bob Perez
Harris Yong

GUST MAE 321: Engineering Design

-Team A-

Randy Chang

Luis Garcia

Robin Liu

Matt Notary

Bob Perez

Harris Yong

12 Jan 1999

Although better than those for the first iteration, second iteration results we again mixed. As before, flow rate exceeded theoretical values, while head was lager than expected. An attempt was made to adjust the length and, therefore, the head, and the best compromise values are shown in Figure 9. One important area of improvement, however, was noise reduction (Figure 10). However, there appears to be a resonance at 4500-5000 rpm. The careful balancing of the motor and fans reduced vibration, and the styrofaooam housing also lowered noise generation. Before the above data were acquired, however, significant work was done to determine the optimum positioning of the two rotors. It was clear that a separation distance of about a half an inch was optimimum, perhaps because placing the second rotor any farther downstream would subject it to the influences of swirling flow. With the half inch spacing, the second rotor was able to increase lift and head over that of one fan alone.

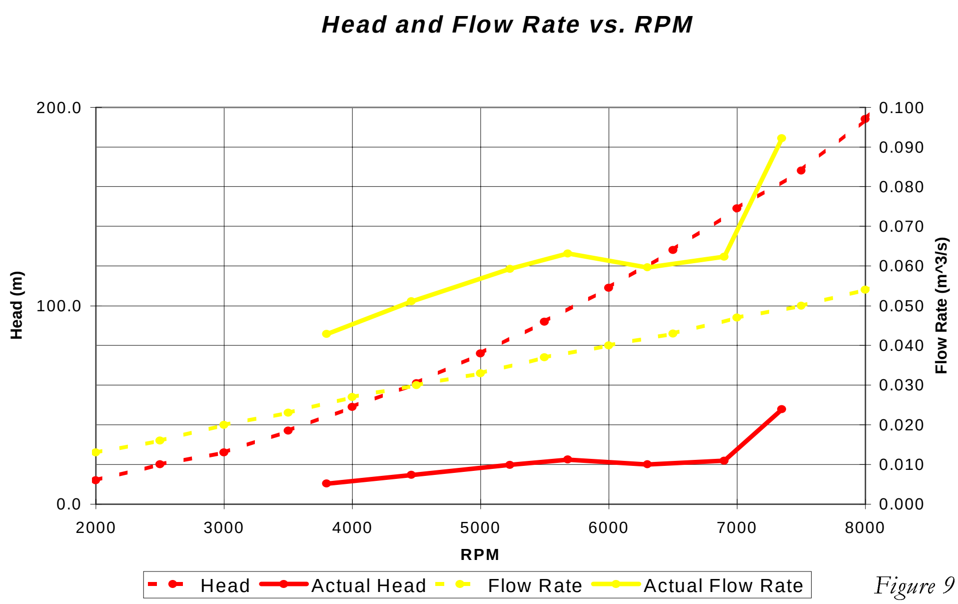

Figure 9

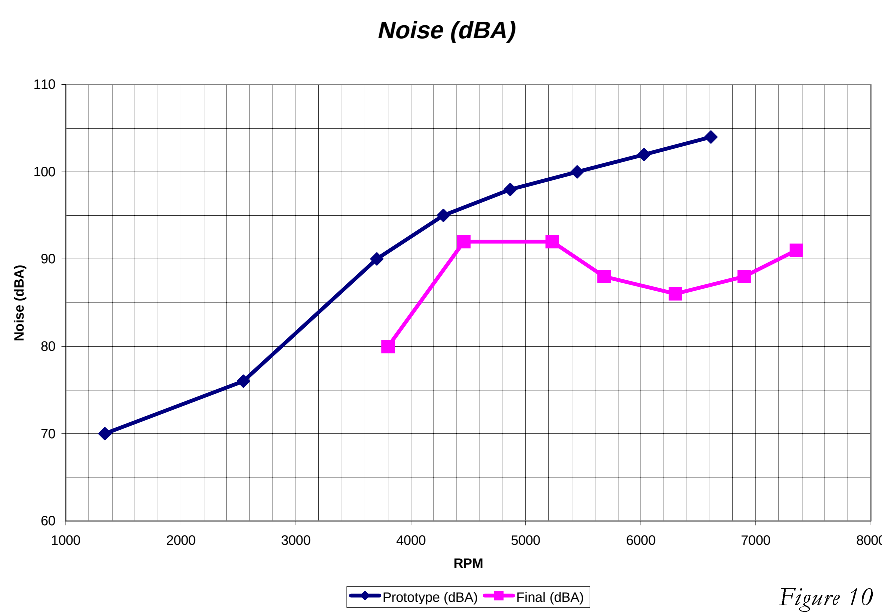

Figure 10

-Team A-
Randy Chang
Luis Garcia
Robin Liu
Matt Notary
Bob Perez
Harris Yong

12 Jan 1999

Further Improvements

The housing design should be improved to decrease weight and increase portability, yet still keep GusT extremely quiet. Fan noise has already been determined to be the main source of noise in the operating unit; noise reduction efforts should be targeted at this section. Specialty insulating material can be considered as a shroud around possible noise sources. One idea involves fabricating a noise reduction composite part consisting of a sound barrier material behind a material designed to absorb noise. The idea governing this design is that noise will travel through the absorber material, lessening in intensity, and then hit the sound barrier material and bounce back into the absorber material, causing more decrease in intensity. Sound insulation is only one of several ways to reduce noise levels in our unit. Work has already been performed on optimizing the dynamic layout in an effort to reduce as much noise-producing friction as possible.

Improving accuracy in the fluid flow model will require additional prototype testing. Actual performance results will be more beneficial than the numerous equations and approximations used in he preliminary calculations. Additionally, designs with more than two axial fans staged in series will be considered. This would reduce the necessary fan diameter and decrease the size of the ducts.

Once a pump design is finalized, a suitable motor that fulfills the power requirements can be custom designed. The universal motor powering the prototype was taken from the competing Toro model. A motor designed to accommodate GusT's load, speed, and torque requirements will allow for tighter overall engineering tolerances and specifications.

Research must also be carried out concerning sources of noise, and more importantly, methods for reducing these sources of noise. Accurate sound measurements and spectral analysis can be performed with the help of Dr. Elizabeth Olsen in the Biophysics Division of the Physics Department at Princeton University.

CONCLUSIONS

Prototype testing has shown great potential for GusT because the main goal of reducing the motor speed while still achieving performance comparable to current leaf blowers was accomplished. Lowering the rotational speed has made GusT significantly quieter. However, there is still room for improvement in many areas, especially in the housing. The enlarged fans require a larger than average housing to accommodate it. Once the fluid dynamics are better modeled, smaller, more efficient fans offering similar performance can be designed. This will reduce unnecessary bulk in the housing to make an already attractive product more appealing.

With these modifications, GusT will be competitive with the leading leaf blower models currently on the market. Furthermore, the revolutionary case design will attract the attention of consumers and prove that performance and aesthetics can coexist in a practical lawn instrument. Unique features such as the interlocking second handle, which allows both left-handed and right-handed people to use GusT with the same ease, and its sleek, ergonomic design will appeal to both those who are shopping for a leaf blower and also those who are just walking down the aisle.

-Team A-
Randy Chang
Luis Garcia
Robin Liu
Matt Notary
Bob Perez
Harris Yong

GUST

MAE 321: Engineering Design

-Team A-

Randy Chang

Luis Garcia

Robin Liu

Matt Notary

Bob Perez

Harris Yong

12 Jan 1999

REFERENCES

Cowles, Geoffrey. Personal Communication.

Hanson. "Noise of Counter-rotation Propellers." *Journal of Aircraft.* 22, 7, 609-17.

Hay, N., R. Metcalfe & J.A. Reizes. "A Simple Method for the Selection of Axial Fan Blade Profiles." *Proceedings of the Institute of Mechanical Engineers.* 192, 25, 269-75.

McQuiston, Faye C. & Jerald D. Parker. *Heating, Ventilating, and Air Conditioning: Analysis and Design.* New York: John Wiley & Sons, 1988.

Northey, Glenn. Personal Communication.

Nosenchuck, Daniel, Prof. Personal Communication.

Parry, A.B. "Modular Prediction Scheme for Blade Row Interaction Noise." *Journal of Propulsion and Power.* 13, 3, 334-41.

Queenan, J. "Turning over a New Leaf." *Chief Executive.* Sep. 96, 117, p. 70

Riegels, F. *Aerofoil Sections.* London: Butterworths, 1961.

Serovy, G.K. "Axial Flow Compressor Aerodynamics." Gordon C. Oates (Ed.), *Aerothermodynamics of Aircraft Engine Components.* Seattle: American Institute of Aeronautics and Astronautics, 1985.

Smits, Alexander, Prof. Personal Communication.

Turton, R.K. *Rotodynamic Pump Design.* Cambridge, 1994.

Vocaturo, Mike. Personal Communication.

Wallis, R.A. *Axial Flow Fans: Design & Practice.* London: Tower House, 1961.

GUST
MAE 321: Engineering Design

-Team A-
Randy Chang
Luis Garcia
Robin Liu
Matt Notary
Bob Perez
Harris Yong

12 Jan 1999

APPENDIX

Operations Flowchart

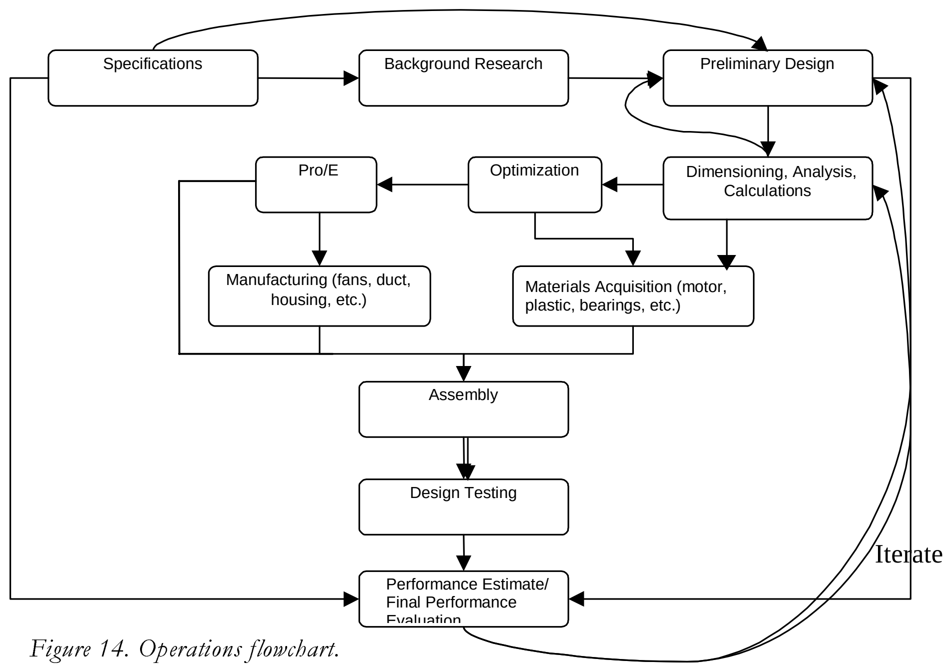

Figure 14. Operations flowchart.

Operations Precedence Matrix